# Segmentation of Periventricular White Matter in Neonatal Brain MRI: Analysis of Brain Maturation in Term and Preterm Cohorts

Alena U. Uus[1(✉)], Mohammad-Usamah Ayub[1], Abi Gartner[2], Vanessa Kyriakopoulou[2], Maximilian Pietsch[2], Irina Grigorescu[1], Daan Christiaens[1,3], Jana Hutter[1], Lucilio Cordero Grande[2,4], Anthony Price[2], Dafnis Batalle[2,5], Serena Counsell[2], Joseph V. Hajnal[1,2], A. David Edwards[2], Mary A. Rutherford[2], and Maria Deprez[1]

[1] Biomedical Engineering Department, School of Imaging Sciences and Biomedical Engineering, King's College London, St. Thomas' Hospital, London, UK
Alena.Uus@kcl.ac.uk

[2] Centre for the Developing Brain, School Biomedical Engineering and Imaging Sciences, King's College London, St Thomas' Hospital, London, UK

[3] Department of Electrical Engineering, ESAT-PSI, KU Leuven, Leuven, Belgium

[4] Department of Forensic and Neurodevelopmental Science, Institute of Psychiatry, Psychology and Neuroscience, King's College London, London, UK

[5] Biomedical Image Technologies, ETSI Telecomunicacion, Universidad Politécnica de Madrid and CIBER-BBN, Madrid, Spain

**Abstract.** MRI is conventionally employed in neonatal brain diagnosis and research studies. However, the traditional segmentation protocols omit differentiation between heterogeneous white matter (WM) tissue zones that rapidly evolve and change during the early brain development. There is a reported correlations of characteristics of the transient WM compartments (including periventricular regions, subplate, etc.) with brain maturation [23,26] and neurodevelopment scores [22]. However, there are no currently available standards for parcellation of these regions in MRI scans. Therefore, in this work, we propose the first deep learning solution for automated 3D segmentation of periventricular WM (PWM) regions that would be the first step towards tissue-specific WM analysis. The implemented segmentation method based on UNETR [13] was then used for assessment of the differences between term and preterm cohorts (200 subjects) from the developing Human Connectome Project (dHCP) (dHCP) project [1] in terms of the ROI-specific volumetry and microstructural diffusion MRI indices.

**Keywords:** Neonatal brain MRI · Periventricular white matter · Brain maturation · Automated segmentation


R. Licandro et al. (Eds.): PIPPI 2022, LNCS 13575, pp. 94–104, 2022.
https://doi.org/10.1007/978-3-031-17117-8_9

## 1 Introduction

Segmentation of T2w structural neonatal brain MRI is conventionally employed in neurodevelopment research studies [9] and there are many existing automated pipelines. These solutions are based on either classical (e.g., label propagation, intensity classification) [6,18,21,26] or deep neural network [10,12] methods. In the majority of these methods, the white matter (WM) is classified as a single tissue component [6,10,18] or subdivided into standard anatomical regions [5,12,21,24] that follow the adult brain parcellation protocols (e.g., temporal lobe, corpus callosum, etc.). However, during the neonatal brain development the WM tissue is highly heterogeneous and constantly evolving due to the different rates of tract maturation and myelination. The example in Fig. 1 shows the regional difference of T2 MRI signal intensities in WM at different ages: 38 to 44 weeks post-menstrual age (PMA). The hyperintense T2 signal regions in WM reportedly correspond the higher water content [11] and are also sometimes referred to as diffuse excessive high signal intensity (DEHSI) ROIs [22] or transient WM [15,23]. These tissue types are transient by nature and eventually are expected to disappear by changing properties and evolving into mature WM tissue. Recently, [23] formalised a new neonatal brain maturation MRI scoring protocol based on the appearance of WM transient compartments including periventricular crossroads, von Monakow WM segments, subplate and germinal matrix. The higher proportion of transient WM are correlated with lower degree of brain maturation. However, apart from the works on segmentation of DEHSI [20,22] or high rate change WM regions [26] that are related to transient WM structures, there has been no reported works on automation of parcellation of specific types of WM tissue defined in [23]. These transient WM ROIs are characterised by the prolonged coexistence in preterm brain [16,23] while periventricular WM is vulnerable to injury [17]. There is also no formalised reference parcellation protocol for transient WM tissue, which is required for development of new automated methods or even simple manual segmentation for quantitative studies.

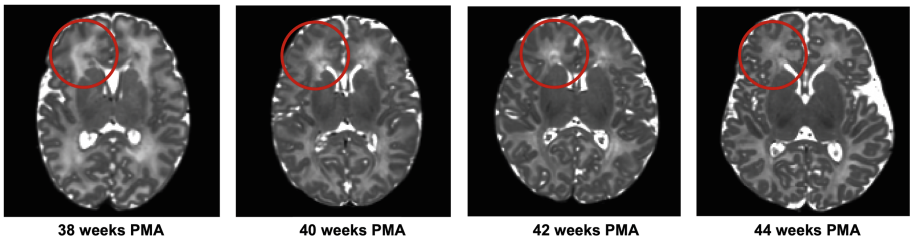


**Fig. 1.** Examples of WM tissue heterogeneity in transient compartments visible on T2w neonatal brain MRI at different PMA (the datasets are from dHCP project [1]).

*Contributions:* In this work, we propose the first deep learning based pipeline for automated segmentation of periventricular white matter (PWM) in neonatal

T2w MRI scans. This extends the already existing solutions [12] for volumetry-based analysis of brain development. The feasibility of the segmentation pipeline is assessed with respect to analysis of the difference between term and preterm cohorts for 200 neonatal subjects from the dHCP project. The PWM segmentations from the proposed pipeline were used for both volumetry and calculation ROI-average microstructural diffusion tensor imaging (DTI) indices.

## 2 Methods

### 2.1 Cohort, Datasets and Preprocessing

The MRI datasets used in this study were acquired as a part of the dHCP project [1] available via the public release. The selected cohort includes 150 term (37–44 weeks gestational age (GA) at birth) and 50 preterm (≤32 weeks GA at birth) neonates scanned between 38 and 44 weeks PMA (Fig. 2). The selection criteria was the absence of major anomalies and good image quality.

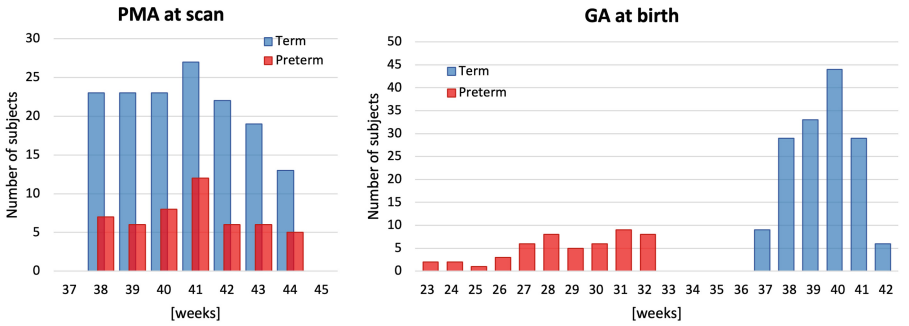


**Fig. 2.** PMA at scan and GA at birth of the investigated neonatal MRI datasets from the dHCP project: term and preterm cohorts.

Each dataset includes diffusion and structural T2w MRI volumes. The acquisitions were performed on a 3T Philips scanner with a 32-channel neonatal head coil and transportation system [14]. The structural T2w volumes were acquired using a TSE sequence with TR = 12 s, TE = 156 ms. The isotropic T2w volumes were reconstructed to 0.5 mm resolution using a combination of motion correction [8] and super-resolution reconstruction [19]. All volumes were N4 bias corrected and normalised in the Draw-EM pipeline [21] that also produced brain tissue parcellation maps. The multi-shell high angular resolution dMRI volumes were acquired with four phase-encode directions on four shells (b-values: 0, 400, 1000 and 2600 s/mm$^2$) with TE = 90 ms, TR = 3800 ms Hutter2018 with 1.5 × 1.5 × 3 mm resolution and 1.5 mm slice overlap and reconstructed to 1.5 mm isotropic resolution using the SHARD pipeline [7] that also includes slice-wise motion correction, distortion correction, exclusion of corrupted slices

and essential preprocessing. The extraction of fractional anisotropy (FA) and mean diffusivity (MD) DTI metrics was performed in MRtrix3 [25] toolbox. The structural to dMRI volumes were co-aligned using T2 to MD affine registration in MRtrix3.

### 2.2 Parcellation Map of Periventricular WM ROIs in the Atlas Space

In order to provide the basis for the automated segmentation pipeline, we defined the first parcellation map of PWM in the MRI atlas space based on the guidance from the clinical MRI studies [15,23]. We used the T2w channel of the 4D neonatal MRI atlas from [26] (36 weeks PMA time-point, 0.5 mm isotropic resolution) as the reference space for segmentation of five periventricular WM regions. The atlas includes the high rate change WM parcellation map, which we subdivided and refined based on the definition of the PWM ROIs (also referred to as "periventricular crossroads") described and illustrated in [15,23]. Refinement was performed manually in ITK-SNAP [2] based on T2 signal intensity boundaries by a researcher with experience in neonatal MRI. The PWM regions were the segmented and named based on the definitions in [23]. This was followed by separation into left and right resulting in ten label ROIs.

### 2.3 Automated Segmentation of Periventricular WM ROIs

To our knowledge, there has been no reported works on automated segmentation of PWM in neonatal brain MRI. The only relevant methods that addressed the tissue-specific delineation of WM were proposed for segmentation of DEHSI [20,22] and high rate change [26] WM regions. These solutions are based on classical intensity thresholding and atlas label propagation, which tend to be prone to errors and sensitive to image quality and preprocessing. This limits their large scale application. As an alternative, we propose to use deep learning for 3D segmentation of multiple PWM regions [23] based on the protocol defined in Sect. 2.2 and [23]. The proposed solution is summarised in Fig. 3.

*Deep Learning Model for Automated PWM Segmentation:* In this work, we used the recently proposed vision transformer based deep neural network segmentation technique (UNETR) [13], as it has shown to perform well for 3D multi-label segmentation. The proposed segmentation pipeline was implemented in MONAI Pytorch-based framework [4]. We selected the default UNETR configuration with combined Dice and cross entropy Loss, AdamW optimiser, $160 \times 160 \times 160$ input size and six output channels (3 left and right PWM regions). For this segmentation network, we selected only the three largest PWM ROIs defined in the atlas space because of the significantly smaller size and lower visibility of the other two regions [23].

*Generations of Labels for Training:* In this case, there were no available manual parcellations of PWM in subject T2w volumes for training due to the time-consuming segmentation of these large regions as well as the difficulty in delineation of not well defined tissue boundaries. Therefore, we created the labels for

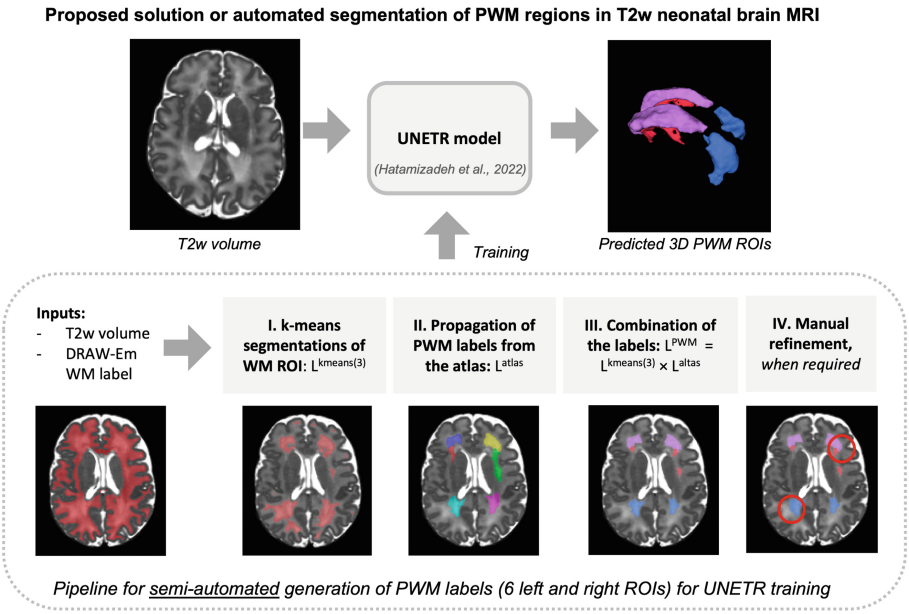


**Fig. 3.** Proposed solution for automated segmentation of PWM in T2w neonatal brain MRI based on UNETR [13] and semi-automated generation of the labels for training.

training of the UNETR network using a semi-automated approach based on the combination of classical methods (see Fig. 3) and manual refinement. At first, kmeans segmentation (from MIRTK toolbox [3]) is used for parcellation of the T2w image within the WM ROI (from the DRAW-EM labels) into 3 clusters. We select only the cluster with the highest intensity. Next, we run propagation of the PWM labels (Sect. 2.2) based on subject-atlas multi-channel registration [26] in MRtrix3 [25]. The output labels of both methods are combined by multiplication. In summary, the label propagation spatially localises and divides the hyperintensity regions detected by kmeans. All steps were implemented based on MIRTK toolbox [3]. We run the label generation pipeline for 80 term and 40 preterm datasets. The output labels were then visually inspected and manually refined in ITK-SNAP, when required.

*Preprocessing and Training of UNETR Segmentation Model:* The preprocessing of the datasets (T2w images and PWM labels) for training included masking using the DRAW-EM brain mask, cropping of the background and resampling with padding to $160 \times 160 \times 160$ grid. We used 90 datasets for training and 10 for validation (including term and preterm). The training was performed for 20000 iterations with the standard MONAI augmentation (random bias field, contrast adjustment, Gaussian noise and affine rotations $\pm 45°$).

*Evaluation of UNETR Segmentation:* The performance was tested on 10 term and 10 preterm datasets qualitatively in terms of the PWM region detection

status (visual assessment: correct = 100%, partial = 50%, failed = 0%), and quantitatively by comparison to the ground truth labels in terms of recall, precision and Dice as well as the relative difference in volume and T2 signal intensity.

### 2.4 Quantitative Analysis of PWM in Term and Preterm Cohorts

The feasibility of using the proposed segmentation pipeline for quantitative studies was assessed based on comparison of term and preterm MRI datasets. We used the trained network to segment 150 term and 50 preterm subjects. The PWM segmentations were used to compute ROI-specific values including volumetry and mean DTI indices (fractional anisotropy (FA) and mean diffusivity (MD)). The scripts for all calculations were implemented in MIRTK toolbox [3].

## 3 Results and Discussion

### 3.1 Parcellation Map of Periventricular WM ROIs in the Atlas Space

Figure 4 shows the first formalised 3D parcellation map for five periventricular WM regions (with left/right separation) along with the original T2w atlas [26]. The segmented regions follow the definitions from [15,23] that call these regions "periventricular crossroads": C1, C2, C4, C5 and C6. The C2 and C5 ROIs have the expected "horn" shape. All PWM ROIs have the pronounced brighter T2 intensity, which is expected to correspond to the higher water content of PWM tissue [15,26]. The segmentations were inspected and confirmed by two clinicians with extensive experience in neonatal brain MRI.

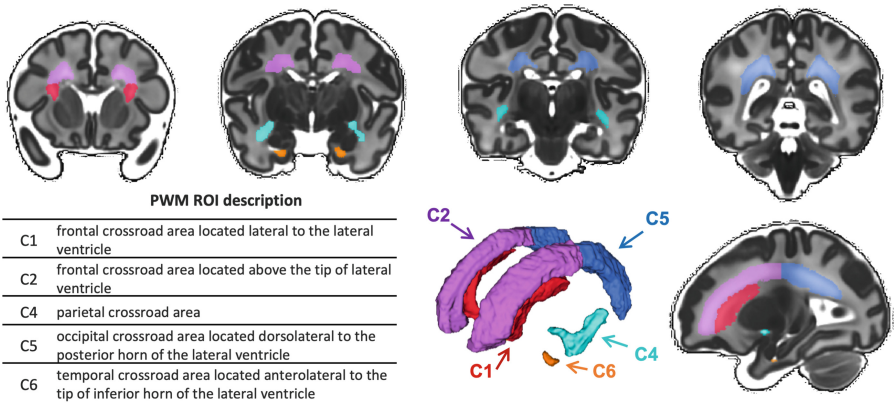


**Fig. 4.** The parcellation map of five periventricular WM regions created in the T2w neonatal brain atlas space [26]. Based on the original definitions in [15,23], these ROIs are referred to as periventricular "crossroads": C1, C2, C4, C5 and C6.

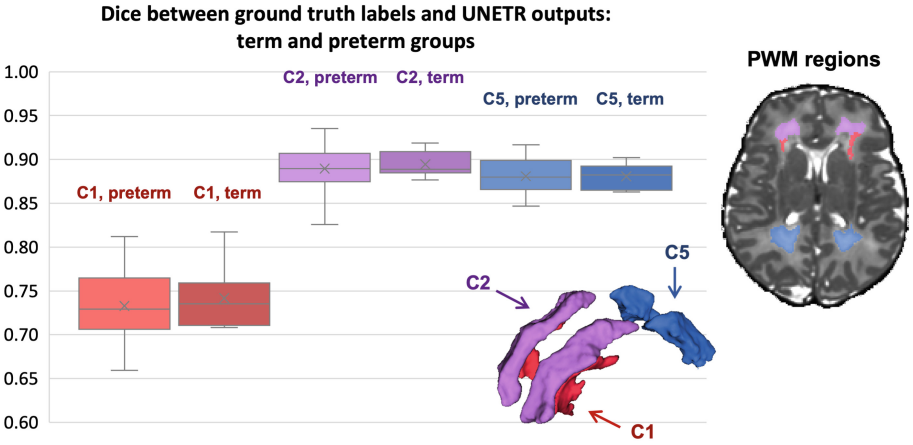


| ROI | Detection status | Dice | Precision | Recall | % volume difference | % intensity difference |
|---|---|---|---|---|---|---|
| PWM C1 | 100 % | 0.74 ± 0.04 | 0.77 ± 0.06 | 0.71 ± 0.08 | 11.01 ± 4.54 % | 1.18 ± 0.99 % |
| PWM C2 | 100 % | 0.89 ± 0.02 | 0.91 ± 0.04 | 0.88 ± 0.05 | 7.09 ± 4.96 % | 0.70 ± 0.99 % |
| PWM C5 | 100 % | 0.88 ± 0.02 | 0.87 ± 0.04 | 0.89 ± 0.04 | 7.14 ± 5.06 % | 0.74 ± 0.98 % |

**Fig. 5.** Quantitative assessment of the trained UNETR model for segmentation of three PWM regions based on the comparison with the ground truth labels on 10 term and 10 preterm test subjects. The metrics (Dice, recall, precision, relative volume and intensity difference) were calculated for combined left and right PWM ROI labels.

### 3.2 Automated Segmentation of Periventricular WM ROIs

The results of testing of the trained UNETR model on 10 term and 10 preterm subjects are summarised in Fig. 5. The network correctly detected all PWM regions selected for training ("crossroads" C1, C2 and C5 as defined in Sect. 3.1 and [23]) in all test subjects (100%). This is confirmed by the relatively high Dice coefficients for all ROIs (around 0.88 for larger PWM ROIs C2 and C5 and around 0.74 for smaller PWM C1) in agreement with the adequate recall and precision. The results are comparable between the term and preterm cohorts. The average relative difference in volume and intensity are 8.42% and 0.87%, correspondingly.

Visual inspection shows that UNETR notably produces slightly smoother labels than the classical methods with smaller volume and slightly higher average intensity with lower standard deviation. However, in this case, we also need to take into account that the ground truth labels are the manually refined outputs of the combined kmeans and label propagation segmentation. Notably, only minimal manual correction was required in 25.4% of all cases primarily when the input WM DRAW-EM labels were incorrect in the ventricle regions and for the late PMA and preterm cases with less pronounced PWM ROIs boundaries. At the same time, neither manual or automated segmentations cannot be

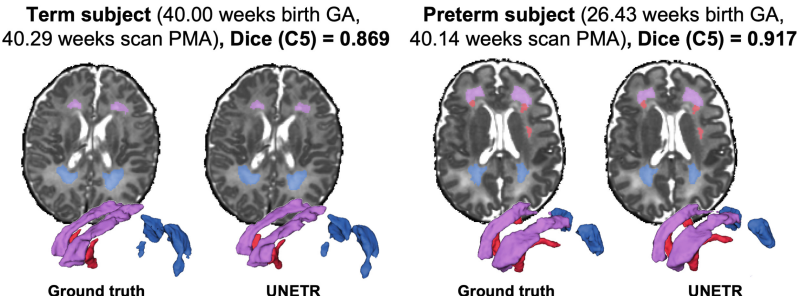


**Fig. 6.** An example of the difference between the ground truth and UNETR output labels for test term and preterm subjects.

considered as the absolute ground truth because there is no precise definition of the correct PWM delineation due to the blurred boundaries, patchy appearance and the transient nature of this WM compartment. This is potentially the main cause of the difference between the ground truth and UNETR label volumes. This is illustrated in Fig. 6 that shows an example of the difference between the ground truth and UNETR output labels for one of the subjects.

### 3.3 Quantitative Analysis of PWM in Term and Preterm Cohorts

Figure 7 shows the results of comparison between 150 term and 50 preterm subjects based on volumetry and diffusion MRI metrics derived from the UNETR PWM segmentations (the analysis was performed for C2 frontal ROI only). All automated segmentations were reviewed and confirmed as acceptable. Additional minor manual refinements were required in 17.5% of cases, which notably did not affect the trends in any of the metrics.

The term cohort is characterised by the pronounced decrease in both absolute and relative PWM volume (that correlates with the increasing total WM volume) along with the decreasing MD and increasing FA, which are the expected changes in maturing WM. On the other hand, there are no prominent (significant) trends for the preterm subjects in any of the metrics. The difference between the term and preterm cohort trends is significant ($p < 0.001$) only in the intensity metrics. The group of preterm subjects have the higher MD and T2 values and lower FA than in the term cohort. This is potentially related to the higher water content due to the prolonged existence of transient WM in the preterm brain [11, 16, 23]. This also is in agreement with the results reported in [26]. However, taking into account the smaller number of available preterm subjects (50), the heterogeneity of the cohort and the respective variations in the GA at birth (24–32 weeks GA, Fig. 2), a more comprehensive investigation on a larger cohort is required for further analysis of correlations between the age at birth and PWM characteristics.

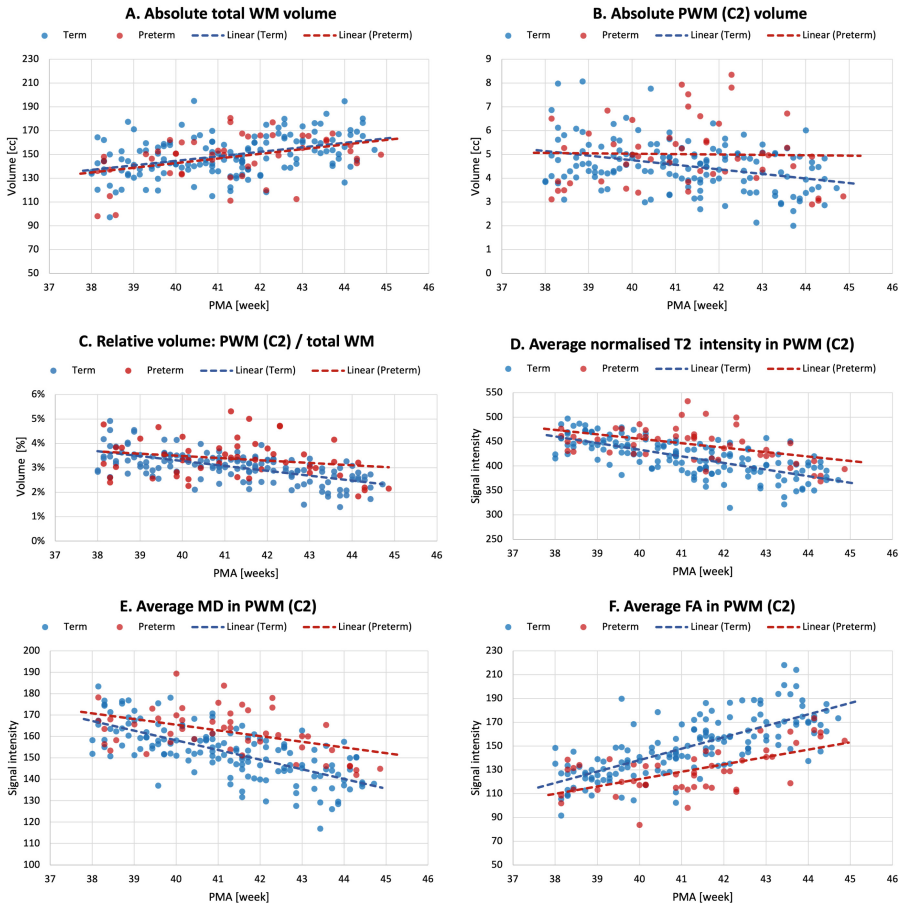


**Fig. 7.** Comparison between term (150, blue) and preterm (50, red) cohorts (dHCP datasets): volumetry and dMRI metrics computed for UNETR PWM segmentations (C2 ROI). (Color figure online)

## 4 Conclusions

In summary, we presented the first deep learning solution for automated multi-label segmentation of periventricular WM regions in neonatal T2w brain MRI. This included formalisation and definition of the PWM parcellation map in the standard atlas space. In addition, we demonstrated the feasibility of using semi-automated combination of kmeans and label propagation for generation of PWM labels for training the of the networks, which significantly decreases the preparation time in comparison to manual labels. The practicability of using deep learning (UNETR) for PWM segmentation was confirmed by quantitative comparison of 200 term and preterm subjects from dHCP cohort. The results of the analysis showed a significant difference in volumetry and mean DTI indices

withing PWM regions. There are also pronounced trends in PWM-derived metrics vs. PMA for the term cohort. Our future work will focus on further automation of parcellation of the rest of the WM tissue types (e.g., subplate), optimisation for different acquisition protocols and wider PMA range and a large scale quantitative analysis.

**Acknowledgments.** We thank everyone who was involved in acquisition and analysis of the datasets as a part of dHCP project. We thank all participants and their families.

This work was supported by the Academy of Medical Sciences Springboard Award (SBF004\1040), the European Research Council under the European Union's Seventh Framework Programme [FP7/ 20072013]/ERC grant agreement no. 319456 dHCP project, the Wellcome/EPSRC Centre for Medical Engineering at King's College London [WT 203148/Z/16/Z)], the NIHR Clinical Research Facility (CRF) at Guy's and St Thomas' and by the National Institute for Health Research Biomedical Research Centre based at Guy's and St Thomas' NHS Foundation Trust and King's College London.

The views expressed are those of the authors and not necessarily those of the NHS, the NIHR or the Department of Health.

## References

1. Developing human connectome project. http://www.developingconnectome.org
2. ITK-snap segmentation tool. http://www.itksnap.org
3. MIRTK Software Package. https://github.com/BioMedIA/MIRTK
4. MONAI Framework. https://github.com/Project-MONAI/MONAI
5. Alexander, B., et al.: White matter extension of the Melbourne children's regional infant brain atlas: M-CRIB-WM. Hum. Brain Mapp. **41**, 2317–2333 (2020)
6. Beare, R.J., et al.: Neonatal brain tissue classification with morphological adaptation and unified segmentation. Front. Neuroinform. **10** (2016)
7. Christiaens, D., et al.: Scattered slice SHARD reconstruction for motion correction in multi-shell diffusion MRI. NeuroImage **225**, 117437 (2021)
8. Cordero-Grande, L., et al.: Three-dimensional motion corrected sensitivity encoding reconstruction for multi-shot multi-slice MRI: application to neonatal brain imaging. Magn. Reson. Med. **79**(3), 1365–1376 (2018)
9. Dubois, J., et al.: MRI of the neonatal brain: a review of methodological challenges and neuroscientific advances. J. Magn. Reson. Imaging **53**, 1318–1343 (2021)
10. Fan, X., et al.: Attention-modulated multi-branch convolutional neural networks for neonatal brain tissue segmentation. Comput. Biol. Med. **146** (2022)
11. Girard, N., et al.: MRI assessment of neonatal brain maturation. Imaging Med. **4**(6), 613–632 (2012)
12. Grigorescu, I., et al.: Harmonized segmentation of neonatal brain MRI. Front. Neurosci. **15**, 565 (2021)
13. Hatamizadeh, A., et al.: UNETR: transformers for 3D medical image segmentation. In: 2022 IEEE/CVF WACV, pp. 1748–1758 (2022)
14. Hughes, E.J., et al.: A dedicated neonatal brain imaging system. Magn. Reson. Med. **78**(2), 794–804 (2017)
15. Judaš, M., et al.: Structural, immunocytochemical, and MR imaging properties of periventricular crossroads of growing cortical pathways in preterm infants. Am. J. Neuroradiol. **26**, 2671–2684 (2005)

16. Kostović, I., Judaš, M.: Prolonged coexistence of transient and permanent circuitry elements in the developing cerebral cortex of fetuses and preterm infants. Dev. Med. Child Neurol. **48**, 388–393 (2006)
17. Kostović, I., et al.: Developmental dynamics of radial vulnerability in the cerebral compartments in preterm infants and neonates. Front. Neuroi. **5**, 1–13 (2014)
18. Kuklisova-Murgasova, M., et al.: A dynamic 4d probabilistic atlas of the developing brain. Neuroimage **54**, 2750–2763 (2011)
19. Kuklisova-Murgasova, M., et al.: Reconstruction of fetal brain MRI with intensity matching and complete outlier removal. Media **16**(8), 1550–1564 (2012)
20. Li, H., et al.: Objective and automated detection of diffuse white matter abnormality in preterm infants using deep convolutional neural networks. Front. Neurosci. **13**, 1–12 (2019)
21. Makropoulos, A., et al.: Automatic whole brain mri segmentation of the developing neonatal brain. IEEE TMI **33**, 1818–1831 (2014)
22. Parikh, N.A., et al.: Automatically quantified DEHSI on MRI predicts cognitive development in preterm infants. Pediatr. Neurol. **49**, 424–430 (2013)
23. Pittet, M.P., et al.: Newborns and preterm infants at term equivalent age: A semi-quantitative assessment of cerebral maturity. Neuroimage **24**, 102014 (2019)
24. Schuh, A., et al.: Unbiased construction of a temporally consistent morphological atlas of neonatal brain development. bioRxiv pp. 2–66 (2018)
25. Tournier, J.D., et al.: Mrtrix3: a fast, flexible and open software framework for medical image processing and visualisation. Neuroimage **202** (2019)
26. Uus, A., et al.: Multi-channel 4d parametrized atlas of macro- and microstructural neonatal brain development. Front. Neurosci. **15**, 721 (2021)